Applied Energy 190 (2017) 1184–1194

Contents lists available at ScienceDirect

Applied Energy

journal homepage: www.elsevier.com/locate/apenergy

A new composite sorbent based on $SrBr_2$ and silica gel for solar energy storage application with high energy storage density and stability

Emilie Courbon [a,*], Pierre D'Ans [b], Anastasia Permyakova [c], Oleksandr Skrylnyk [a], Nathalie Steunou [c], Marc Degrez [b], Marc Frère [a]

[a] Department of Thermodynamics and Mathematical Physics, Université de Mons, Boulevard Dolez 31, B-7000 Mons, Belgium
[b] 4MAT Department, Université libre de Bruxelles (ULB), Avenue F.D. Roosevelt, 50 - CP 194/3, B-1050 Bruxelles, Belgium
[c] Institut Lavoisier, Université Versailles-Saint-Quentin-en-Yvelines, Université Paris Saclay, 45 Avenue des Etats-Unis, 78035 Versailles Cedex, France

HIGHLIGHTS

- Synthesis of a new composite material based on $SrBr_2$ and silica gel.
- High energy storage density of 203 kW h/m^3 is reported for thermal energy storage applications.
- High cycling stability is reported.

ARTICLE INFO

Article history:
Received 10 October 2016
Received in revised form 21 December 2016
Accepted 15 January 2017

Keywords:
Composite
Silica gel
Strontium bromide
Sorption isotherms
Energy storage

ABSTRACT

The excellent matching between the sorption and desorption temperatures of hexahydrated $SrBr_2$ and those required for solar heat storage for building applications, the high heat of reaction (67.5 kJ/mol of water) coupled with the gain/loss of 5 mol of water per mole of salt make this salt an appealing sorbent for solar thermal energy storage applications coupled to space heating. Due to the morphological instability of this salt, it is necessary to incorporate it in a porous matrix as a composite sorbent. A new composite material for thermochemical energy storage applications was developed. It consists of a mesoporous silica gel impregnated by strontium bromide with salt content equal to 58 wt.%. The structure and the sorption properties of the composite were characterized by SEM-EDX, temperature dependent XRD, XRF, and N_2 sorption measurements. The salt is homogeneously distributed inside the pores of the silica gel. Water sorption isotherms were measured between 20 °C and 80 °C, which enabled us to understand the sorption mechanism. A mathematical model was developed and used to fit the experimental data in order to predict the sorption behavior of the composite at different conditions (influence of temperature and pressure conditions on the cycle loading lift and energy storage density). The interest of using such a composite for thermal energy storage application is then discussed (thermal energy produced by solar collector and used for space heating). A high cycle loading lift of 0.22 g/g is obtained corresponding to an energy storage capacity of 230 W h/kg and an energy storage density of 203 kW h/m^3 of packed bed composite (between 30 °C and 80 °C at 12.5 mbar) is reported, with an excellent stability over 14 sorption/desorption cycles. The sorption kinetics of this composite is enhanced compared to pure salt. Test on a laboratory scale open type reactor gives a maximum specific thermal power of 200 W/kg and a mean specific thermal power of 92 W/kg at 30 °C and 12.5 mbar for an extent of reaction of 0.68.

1. Introduction

Nowadays it is increasingly important to improve the share of renewable energies in final energy consumption in order to reach the objectives defined by the European Commission (20% of final energy produced from renewables in 2020, and 27% in 2030). Solar energy is one of the most interesting solutions among renewable energy resources as it can be converted easily into heat or electricity. The main problem when using such an energy source is its unfair time distribution, which may cause a mismatch between needs and availability. Seasonal storage of solar energy is required to collect energy during summertime to be used in winter. The need for seasonal solar thermal energy storage systems is crucial

* Corresponding author.
E-mail address: Emilie.courbon@umons.ac.be (E. Courbon).

http://dx.doi.org/10.1016/j.apenergy.2017.01.041
0306-2619/

for space heating application in temperate and cold climate countries. The relevance of such a technology is even more stringent in EU28 which adopted a regulation called Nearly Zero Energy Building Directive to be effective in 2020 for new buildings [1]. The low energy consumption of these new buildings (e.g. 3000 kW h/year for space heating of a 100 m^2 dwelling in Belgium) will have to be mainly covered by local renewable energy sources. In countries with high heat demand buildings, the optimal solution is to use a heat pump while the electricity consumption is totally covered by PV production. To avoid massive electricity production/consumption during summer/winter, a more elegant solution would be to avoid the electrification of the heat demand by using thermal solar collectors and seasonal heat storage [2]. Seasonal heat storage for space heating is not considered as a completely mature technology. It requires to store huge energy quantities during several months with reduced losses to be recovered later on at a temperature level which fits the application. Up to now, demonstration cases [3] were developed relying on sensible heat technologies (water tanks, gravel pits, aquifer and underground energy storage); the heat storage system is centralized at the level of a district thus requiring a district heating grid. One of the most well-known case is the Drake Landing Solar Community which reaches a 100% solar coverage of the heating needs of a 52-dwelling district in 2015–2016 [4]. It uses a 30,000 m^3 underground heat storage with an energy density of approximately 25 kW h/m^3. In order to reduce costs and size of seasonal heat storage systems, higher energy densities are required, which is not possible when considering sensible heat storage technologies. Thermochemical storage technologies (sorption systems) present high theoretical energy storage densities (up to several hundreds of kW h/m^3) and low losses (energy is stored through chemical bonds rather than through temperature lift). This is in accordance with long term energy storage requirements, particularly when a chemical sorbent is used [5–8]. In sorption systems, during summer, the energy is stored thanks to the desorption process, which needs heat provided by the solar collectors, whereas during winter, the heat is produced by the adsorption process, which is exothermic.

While thermochemical storage is a promising technology for ensuring a 100% solar coverage of the heat demand in buildings through seasonal operation, its Technology Readiness Level (TRL) remains low (4–6). Further developments are needed in terms of storage material, reactor and system for first demonstration cases to be developed [9,10]. In terms of storage material, high energy storage density (kW h/m^3) or/and storage capacity (W h/kg) are the key parameters to consider, as well as non-toxicity, availability and cost [11,12]. An energy storage density at equilibrium of 150 kW h/m^3 may be considered as a minimum target value to ensure a real breakthrough compared to sensible heat storage. High cycling stability is another crucial parameter for long life operation of the system (at least 25 cycles). Reactor design must be performed in such a way that the maximum heat flow to be stored during summertime and provided during wintertime for ensuring internal thermal comfort may be effectively stored/produced. Thermochemical systems generally exhibit high kinetics at the starting point of the reaction and a poor one when approaching equilibrium. One of the main challenges when designing the reactor is to bring the system close to equilibrium for ensuring a high energy storage density while keeping the reactor size acceptable. In terms of system, the main challenge is to size all the components (solar collector surface area, heat emission system within the building) so that the reactor/whole system may operate in favorable conditions (conditions that foster the global system performance: e.g. low heat emission temperature, optimized desorption temperature for maximizing both the energy storage density and the solar collector efficiency). These challenges must be performed in an integrated way [13]. For example, the energy storage density at equilibrium of a given storage material depends on the conditions of use of the system (e. g. temperatures at which the heat must be stored/recovered). Those conditions mainly depend on the different components of the complete storage system (type of solar collector, heat distribution system within the house, closed or open reactor). Assuming too optimistic conditions could lead to consider a material as promising without any guarantee of success once tested at the prototype level.

This research work mainly focuses on the development of a new storage material for thermochemical storage (solar heat for space heating application) while taking into account all the required specifications for a final use in a heat storage prototype (e.g.: high energy storage density in working conditions close to the application, high cycling stability and appropriate kinetics).

Concerning the storage material, chemical sorbents that were identified for solar thermal energy storage/space heating applications are inorganic hydrated salts which present some disadvantages when used as pure materials. For example, the hydration/dehydration process may produce the swelling of the salt, due to a change of crystal structure, which may limit the heat and mass transfers [14]. A hard crust is also observed for some inorganic salts due to the agglomeration of partially hydrated salt. This problem was observed for example for $MgCl_2$, $MgSO_4$ [15], $CaCl_2$ [16] and $SrBr_2$ [17]. Problems of aggregation or pulverization are also observed when a salt is used in a thermochemical storage reactor [18]. Concerning chlorides, they tend to form a gel-like substance due to the melting of the hydrated salt [19]. In order to limit those problems, the salt may be confined into the pores of a porous matrix and hence used as a composite sorbent [20, 21]. Composite sorbents are expected to exhibit in-between sorption properties compared to the physical adsorbent used as the porous matrix and the inorganic salt. As a consequence, one could control the sorption capacity by varying the porous matrix structure, the chemical structure of the hydrated salt and/or the amount of salt inside the pores.

When stabilizing a salt by the synthesis of a composite, a compromise must be found between the incorporation of a high salt content into the pores of the matrix to keep a high energy storage density, and a good stability of the composite material under successive hydration/dehydration cycles. The synthesis procedure must be optimized for such an objective and rely on a comprehensive set of structural data that allow us to evaluate the long term stability of the composite. Structural data may also be used, together with energy performance measurements in a wide range of conditions, to propose the sorption mechanism and hence, a reliable model for sorption properties calculation to be used as a tool for engineers.

In the present study, a new composite based on $SrBr_2$ and silica gel was synthesized in order to stabilize the salt and to facilitate its future use in seasonal storage system for space heating application. The choice of the salt and the matrix was based on a literature review which will be detailed in the following section. In order to increase the composite cycling stability, a new and original synthesis protocol was developed, which allowed us to reach a high salt content, homogeneously distributed into the pores of the matrix. The composite structural and sorption properties were determined. The efficiency of this material for solar storage applications was evaluated on small samples (a few tenth of mg) by measuring the cycle loading lift, the energy storage density and the cycling stability, in conditions close to the real ones in terms of temperature and pressure. The adsorption temperature was set to 30 °C, while the desorption temperature was set to 80 °C, easily reachable with thermal solar collectors. For both adsorption and desorption steps, the water vapor pressure was set to 12.5 mbar, corresponding to the saturation vapor pressure at 10 °C, representative of condensation or evaporation conditions

in a closed system, and also to 50% relative humidity at 20 °C, representative of conditions in an open system. These tests conditions are realistic. The desorption temperature is voluntarily low, compared to the state of the art, where desorption temperatures between 120 and 150 °C were preferred. A mathematical model fitting the experimental sorption data enabled to study the influence of parameters such as temperature and pressure on the cycle loading lift and on the energy storage density. Kinetics of adsorption for composite and for pure $SrBr_2$ were evaluated in order to qualitatively assess the effect of salt impregnation: kinetics in the composite material appeared to be enhanced compared to the pure salt in the same conditions. Finally, the composite was tested in a laboratory open type thermal storage prototype. These tests allow us to study the kinetic behavior of the composite in aeraulic conditions that are close to the application ones. They provide results for easy scaling up to real size equipment.

2. State of the art: selection of salt and information about reported composites

Composite sorbents have attracted great attention for two solar thermal energy storage applications: sorption heat pumping applications for which high mass uptake and fast kinetic are required to obtain high thermal power [22,23]; and thermochemical storage applications (middle or long-term storage) for space heating or refrigeration, for which high energy storage density (expressed in kW h/m^3) is required to limit the volume of material needed to cover the energy demand of the building [5,24]. Depending on the intended application, the required properties of the composite material are different: while the mass uptake and kinetics are crucial criteria for heat pumping application, the energy storage density (kW h/m^3) or the storage capacity (W h/kg) are the key parameters to consider for heat storage application.

State of the art in terms of composite materials for thermochemical storage must be carried out with care as discrepancies in tests conditions may lead to the impossibility of comparing the performance results. Previous and current developments mainly focus on silica gel, activated carbon or zeolite as porous matrix, and on $CaCl_2$, $Ca(NO_3)_2$, $MgSO_4$, LiBr or LiCl as inorganic salt. Vasiliev et al. [25] developed a composite based on active carbon fibre and 95 wt.% $CaCl_2$ in reaction with ammonia for heat pumps and refrigerators. Wu et al. [26] studied the synthesis of $CaCl_2$/silica gel composites and evaluated the influence of the physico-chemical parameters (salt concentration of the aqueous solution, temperature and duration of impregnation) on the amount of $CaCl_2$ incorporated into the pores of silica gel and on the sorption properties of composites. Authors found that the composite impregnation from a solution of $CaCl_2$ at 30 wt.% leads to a high storage capacity of 283 W h/kg at the desorption temperature of 90 °C. As Gordeeva et al. [27] explained, the method of preparation of the composite impacts its final composition. Simonova et al. [28] developed a composite based on silica gel and $Ca(NO_3)_2$ which adsorbs around 0.20 g of water/g anhydrous sorbent at 12.4 mbar and 35 °C. To evaluate the performance of this composite for air conditioning applications, the cycle loading lift between the hydrated state at 30 °C and 9 mbar and the dehydrated state at 80 °C and at 45 mbar was calculated. It appeared to be equal to 0.17 g/g which corresponds to a storage capacity of 111 W h/kg of anhydrous composite. Tretiak and Abdallah [29], and Jänchen et al. [30] studied the impregnation of $CaCl_2$ in different types of clay. The composite attapulgite/$CaCl_2$ studied by Jänchen et al. adsorbed 0.40 g/g at 23 °C and at 8.4 mbar, and reached a storage capacity of 242 W h/kg of anhydrous composite at 40 °C and 20 mbar. Ji et al. [31] studied the efficiency of a composite based on $CaCl_2$ incorporated into the pores of the Mobil Composite Material MCM-41 for solar-driven fresh water production. This composite adsorbed up to 1.75 g water/g of anhydrous sorbent at 10–15 °C and at a relative humidity ranging from 78% to 92%; around 90% of the sorbed water could be removed at 80 °C. However, a deterioration of the performance was observed after more than 10 sorption/desorption cycles. Hongois et al. [32] chose to develop a composite based on zeolite 13X and $MgSO_4$, which adsorbed 0.14 g/g at 30 °C and 17–19 mbar. The storage capacity of this composite was 180 W h/kg (which corresponds to an energy storage density of 166 kW h/m^3). Ristic et al. [33] developed a composite based on $CaCl_2$ and FeKIL2 with 7 wt.% of $CaCl_2$, this composite presented a loading lift of 0.20 g/g and an energy storage capacity of 560 kJ/kg (155 W h/kg) with adsorption at 25 °C and 12 mbar and desorption at maximum 150 °C and 56 mbar. This composite showed a 3.6% loss of water uptake capacity after 20 cycles. Zhang et al. [34] developed a composite based on $SrBr_2$ and expanded vermiculite, which contained 63 wt.% of $SrBr_2{\cdot}H_2O$ (corresponding to 59 wt.% of $SrBr_2$), they measured a mass uptake at 30 °C and 2545 Pa of 0.53 g/g which corresponded to an energy storage capacity of 460 W h/kg and an energy storage density of 105 kW h/m^3. Despite a high salt content, this composite does not reach a high enough energy storage density for solar heat storage coupled to space heating application.

Even if the test conditions are different in these different studies, it gives an order of magnitude of the performances that a new composite should reach to be competitive compared to the state of the art. It must be noted that strontium bromide is considered in only one study devoted to composites (low energy density was reached in favorable conditions), whereas it has promising properties for solar heat storage for low energy building space heating application [35–37]. The reaction which occurs in the conditions of use of heat storage systems (adsorption temperature = 30 °C, desorption temperature = 80 °C, water vapor pressure = 12.5 mbar,) is the following one:

$$SrBr_2 \cdot H_2O + 5\ H_2O \leftrightarrow SrBr_2 \cdot 6H_2O + \text{heat} \qquad (\Delta H = 67{,}460\ \text{J/mol}\ H_2O)$$

The high enthalpy of reaction (ΔH = 67,460 J/mol H_2O) and the density of the hexahydrated strontium bromide (2.386 g/cm^3) allow the salt to reach a high energy storage density of 629 kW h/m^3 of hexahydrated strontium bromide. The hexahydrated form of the salt is taken as reference as the volume of the hydrated salt is nearly two times higher than the one of the anhydrous salt. Thanks to a high melting point (88.6 °C for $SrBr_2{\cdot}6H_2O$), no problem of salt melting is expected to occur in the storage process. Literature shows that strontium bromide has already been investigated at the prototype level which is not the case for most of the composites presented previously. Michel et al. [37] obtained a packed bed energy storage density of 388 kW h/m^3 for the use of $SrBr_2$ in an open reactor. The thermodynamic efficiency of $SrBr_2$ was already proven by previous studies, but in most cases $SrBr_2$ was mechanically mixed with expanded natural graphite to limit problems due to volume change during the hydration/dehydration process [38–40]. Mauran et al. [40] evaluated the consolidated $SrBr_2$ in a 1 m^3 prototype able to store 60 kW h. Zhao et al. [41] developed a consolidated $SrBr_2$ with expanded natural graphite treated with sulfuric acid (ENG-TSA) for which they obtained an energy storage density of 185 kW h/m^3, this composite was tested in a 1 kW h closed reactor. Fopah Lele et al. [17] evaluated the efficiency of $SrBr_2$ used as pure salt in a closed system with a honeycomb heat exchanger, to limit the problem of salt agglomeration. For waste heat recovery application, they obtained a reactor energy storage density of 115 kW h/m^3 based on their simulation work. The use of pure salt exhibits morphological problems that should be solved, mechanically (improving the design of the heat exchan-

ger [17]) or by adding a new material (expanded natural graphite [38–40]). Another solution to stabilize the salt would be to incorporate it into the pores of a porous matrix. The composite should exhibit high sorption capacity and energy storage density in the conditions of use of a storage system for space heating application.

Considering the state of the art in terms of composite materials for heat storage and the use of $SrBr_2$ in prototypes, we propose to develop a new composite material, based on $SrBr_2$ incorporated into the pores of silica gel. This composite should allow us to avoid morphological changes that are encountered when using the pure salt, while benefiting from the high energy storage density of $SrBr_2$. The mesoporosity of silica gel should facilitate the incorporation of high salt content while keeping an easy access for water vapor to the salt, ensuring both high sorption performances and high cycling stability. Considering the best in kind composite that has been investigated for long term solar energy storage for building application (Zeolite 13X/$MgSO_4$), the targeted value of the energy storage density to be reached or overpassed is 166 kW h/m^3.

To the best of our knowledge, no composite based on the incorporation of strontium bromide into the pores of silica gel has been developed and studied so far. The targeted minimum energy storage density should be reached for realistic but not too favorable temperature and pressure conditions (pressure = 12.5 mbar, adsorption temperature = 30 °C and desorption temperature = 80 °C); namely the desorption temperature is not too high. To ensure both high energy density and long term stability and composite homogeneity, a new synthesis protocol is proposed; it is based on maximizing the salt content while ensuring stability and homogeneity by successive salt loading in the matrix. This paper also intends to provide a comprehensive set of data. Structural data will help to assess the homogeneity of the composite and to qualitatively evaluate its long term stability. Sorption data will be used for determining the energy storage density at equilibrium and cycling stability. Tests in a laboratory heat storage prototype (reactor), using air as a heat and water vapor carrier fluid, was performed to evaluate the system dynamic in aeraulic conditions close to the final application.

The ambition of this paper is thus to provide a new composite material for solar heat storage and space heating application, with enhanced performance compared to the state of the art, its preparation method and a comprehensive set of data that makes possible its successful use in a real scale heat storage prototype.

3. Materials, synthesis and characterization

The porous matrix is silica gel Davisil grade 62 from Grace, labelled SG62 in this article. This silica gel contains mainly mesoporosity with disperse pore sizes. The hexahydrated strontium bromide with a purity of 99% was provided by Sigma Aldrich.

The composite was synthesized by using incipient wetness impregnation method with successive impregnation/drying steps.

The silica gel (300 g) was dehydrated in an oven at 200 °C for 4 h until the mass remains constant (anhydrous mass = 290 g). The matrix was then cooled down to ambient temperature before salt loading. A volume of an aqueous solution of $SrBr_2$ at 40 wt.%, V_{sol}, corresponding to the pores volume of silica gel sample, was added to the matrix and mixed to homogenize the mixture. The volume of solution is calculated by Eq. (1).

$$V_{sol} = V_{p_{matrix}} \times m_0 \quad (1)$$

With $V_{p_{matrix}}$ the pores volume of the silica gel and m_0 the mass of anhydrous silica gel. In present case, V_{sol} = 333 mL.

The silica gel was impregnated for 1 h at ambient temperature. Then the mixture was dried in an oven at 200 °C for 1 night to evaporate the remaining water. The salt content, SC, can be calculated by Eq. (2):

$$SC\ (\%) = \frac{m_1 - m_0}{m_1} \times 100 \quad (2)$$

With m_1 the mass of the dehydrated composite (silica gel + $SrBr_2$), and m_0 the mass of anhydrous silica gel.

A second impregnation step with the addition of 333 mL of salt solution was done, followed by a drying step at 200 °C overnight. The final salt content is calculated by Eq. (2).

The impregnation step and the drying step were repeated as many times as necessary to reach the desired salt content, following patent WO/2015/197788 [42].

The salt content was checked by X ray fluorescence using a Pioneer S4 (Bruker) device. Since the oxygen measurement is not precise, it is assumed that O is linked to Si as SiO_2 and that the overall material is dry. Other elements are considered independently.

The specific surface area, the total pore volume and the average pore diameter of the composite were determined through nitrogen sorption measurements at 77 K using a Belsorp max apparatus and using the BET method. Prior to nitrogen sorption measurements, the sample was dried at 200 °C under vacuum for 10 h. The specific surface area was calculated using the branch in the relative pressure range between 0.05 and 0.22 for silica gel and between 0.05 and 0.17 for SG62/$SrBr_2$ composite. The total pore volume was estimated from the amount adsorbed at relative pressure of 0.99. The average pore diameter was calculated with the hypothesis that the pores are cylindrical. The external surface area and the primary mesopore volume were obtained thanks to the α_s-plot method from the adsorption data in the range of α_s from 4.27 to 7.07 for silica gel and from 3.58 to 7.07 for SG62/$SrBr_2$ composite. The micropore volume was estimated by the same α_s-plot method from the adsorption data but in the range of α_s from 0 to 0.95 for silica gel and from 0 to 1.24 for SG62/$SrBr_2$ composite [43,44]. The pore size distribution was obtained by the Barrett, Joyner and Halenda (BJH) method applied on the nitrogen desorption isotherm.

The composite was analyzed in cross-section by Scanning Electron Microscopy (SEM) with a FEI Quanta 3D® and EDAX® analyzer. In order to obtain cross-sections, particles were trapped inside a metallographic resin. The resin was then polished using SiC paper, until several particles were reached. Then, the surface of the cross-section was more finely polished using diamond paste and diethylether to form a slurry that does not dissolve $SrBr_2$. After depositing a conductive layer, analyses of composition at the center and outside the particle were made, with a comparison between inner and outer squares of analyses. These squares were obtained based on a rectangle aspect ratio 10:1 inscribed in the cross-section.

The particle size distribution was evaluated by laser diffraction with a dry dispersion on Malvern Master Sizer 3000 with a 300F lens enabling to measure particle size between 0.5 and 900 μm.

X-ray thermodiffractometry (XRTD) was performed under air, in a Bruker D8 advance diffractometer using Cu Kα radiation (λ = 1.7903 Å). The temperature range is 30–170 °C with measurements every 10 °C. Between measurements, the temperature increasing rate is 2 °C min^{-1}. The 2θ angle was varied from 8° to 60° by steps of 0.02°, 2 s/step. Prior to the measurements, the composite was hydrated under saturated water atmosphere for about 70 h in order to form initially the $SrBr_2 \cdot xH_2O$ (x > 6) phase in the pores of the composite (water content: 0.69 g/g).

The water sorption isotherms were measured with a dynamic vapor sorption apparatus, IGASorp from Hiden Isochema between 20 °C and 80 °C, in the presence of water vapor supported by nitrogen with a flow rate of 250 mL/min. Prior to the measurements, the sample was dried at 200 °C for 10 h under dry nitrogen at atmospheric pressure.

The efficiency of the composite for heat storage application was evaluated on TG-DSC 111 coupled with a humidity generator Wetsys from Setaram with nitrogen as inert gas. The flow rate of humid nitrogen was 50 mL/min. Prior to analysis, the sample was dried at 200 °C under vacuum for 10 h. The sample was first hydrated at 30 °C and 12.5 mbar (corresponding to saturation pressure at 10 °C) and then heated at 80 °C at 12.5 mbar. The mass change (in gram of water per gram of anhydrous composite) between 30 °C and 80 °C at 12.5 mbar corresponds to the cycle loading lift of the composite. The heat of sorption is obtained by integrating the heat flow signal. As the experiment is realized under a change of temperature, one has to take into account the heat needed to heat the crucibles and the sample. The heat of sorption is then calculated as followed:

$$\Delta H_{sorption}(J/g) = (\Delta H_{exp}(mJ) - \Delta H_{crucible}(mJ) - mc_p\Delta T(mJ))/m(mg)$$

where ΔH_{exp} is the integration of the heat flow signal during the test on the composite, $\Delta H_{crucible}$ is the integration of the heat flow signal during a blank test (empty crucibles), m is the anhydrous sample mass, c_p is the heat capacity of the composite and ΔT is the difference of temperature of the sample (here 50 °C).

Thanks to an experimental measurement of the packing density of the composite, one can calculate the energy storage density in kW h/m^3.

The stability of the composite under 14 successive sorption/desorption cycles was evaluated using the same device, by repeating the sorption/desorption cycles.

Kinetics of adsorption were measured on TG-DSC 111 coupled to a humidity generator Wetsys from Setaram between 80 °C and 30 °C at 12.5 mbar. Concerning $SrBr_2$, 84.6 mg of $SrBr_2{\cdot}6H_2O$ (corresponding to 58.87 mg of $SrBr_2$) were first heated to 80 °C at 12.5 mbar of water partial pressure (nitrogen as inert gas at 50 mL/min) and then the adsorption step is measured by changing the temperature from 80 °C to 30 °C, keeping the same water partial pressure. Concerning the composite, the sample is first dried under vacuum for 10 h, the anhydrous mass is 54.85 mg. The sample is then submitted to the efficiency test (adsorption at 30 °C and 12.5 mbar, desorption at 80 °C and 12.5 mbar). The kinetics is then measured by changing the temperature form 80 °C to 30 °C at 12.5 mbar of water partial pressure.

The SG62/$SrBr_2$ composite was evaluated in a laboratory scale open sorption prototype with a humid flow rate of 215 mL/min. Tests were run on 245 g composite with a 10 mm height layer in the column. The temperature was set to 30 °C and the water vapor pressure to 12.5 mbar. The test bench allows the measurement of the outlet air temperature and humidity as well as the mass change of the composite with time.

4. Results and discussion

The salt content of the anhydrous composite measured by X ray fluorescence is 59 ± 2 wt.% which is in fair agreement with the salt content determined by the mass difference of samples before and after salt encapsulation (i. e. SC = 58 wt.%) (Table 1).

Concerning the nitrogen sorption measurement (Fig. 1), both silica gel and SG62/$SrBr_2$ 58 wt.% composite exhibits adsorption isotherms typical of mesoporous materials with capillary condensation at high relative pressure. The hysteresis between adsorption and desorption branches occurs in a narrow pressure range. The presence of $SrBr_2$ slightly modifies the hysteresis loop, with a closure point at higher relative pressure compared to pure silica gel. This highlights an increase of the pore diameter which is consistent with the pore size distribution obtained by BJH method (Fig. 2). This confirms the incorporation of salt into the pores of the matrix, the salt completely filled the smallest pores of the matrix and partially filled the largest pores of the matrix. Nevertheless, the apparition in the composite of larger pores than in the matrix is surprising. This could be explained by a different interaction between N_2 molecules and the surface of composite containing salt which could interfere with the pore size calculation.

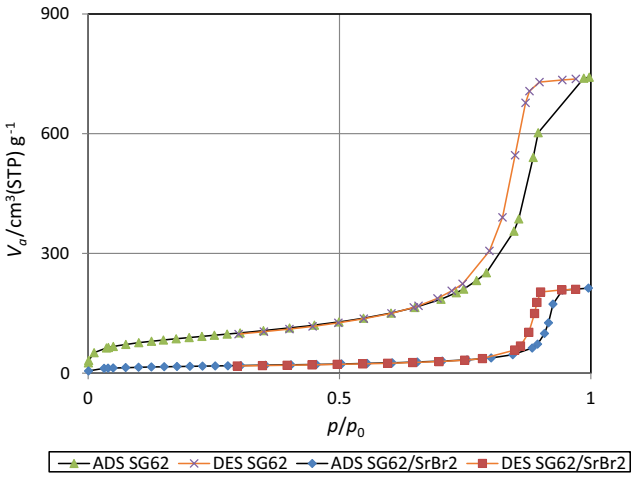

Fig. 1. Comparison of N_2 adsorption (black line) and desorption (orange line) isotherms at 77 K of silica gel (violet cross and green triangles) and composite SG62/$SrBr_2$ 58 wt.% (blue diamond and red squares). (For interpretation of the references to colour in this figure legend, the reader is referred to the web version of this article.)

In comparison to the pure porous matrix (Table 2), a significant decrease of both the specific surface area and the total pore volume of the composite is observed in agreement with the incorporation of the salt into the pores of the silica matrix. The primary mesopore volumes obtained by α_s-plot method are very close to the total pore volumes obtained by BET analysis, which confirmed that silica gel and SG62/$SrBr_2$ 58 wt.% composite are both mainly mesoporous. Both silica gel and SG62/$SrBr_2$ 58 wt.% composite do not present any micropore volume. In comparison to the pure silica gel, a small decrease of the external surface area is observed, indicating the possible presence of a small amount of salt into the macropores or onto the surface of the matrix. This could lead to a problem of stability of the composite. That is why the cycling stability of the composite will be controlled in the present work, before a potential use in a storage system.

Knowing the pore volumes of the matrix and composite, the salt content can be calculated considering that the salt occupies the pores of silica and thus the difference of volume between the matrix and composite. This salt content, SC_{BET}, is calculated by the following equation, with $V_{p_{matrix}}$ the pore volume of silica gel (cm^3/g), $V_{p_{composite}}$ the pore volume of the composite (cm^3/g) and ρ_{salt} the density of anhydrous $SrBr_2$ (4.216 g/cm^3):

Table 1
XRF analysis of the composite.

	SiO_2	Br	Sr	Ca	Cl	S	Cu	Fe	Cr
Weight%	40.41	39.73	19.73	0.0506	0.034	0.021	0.013	0.0082	0.0057
Equipment error	0.12	0.007	0.008	0.0028	0.004	0.003	0.0008	0.0007	0.0011

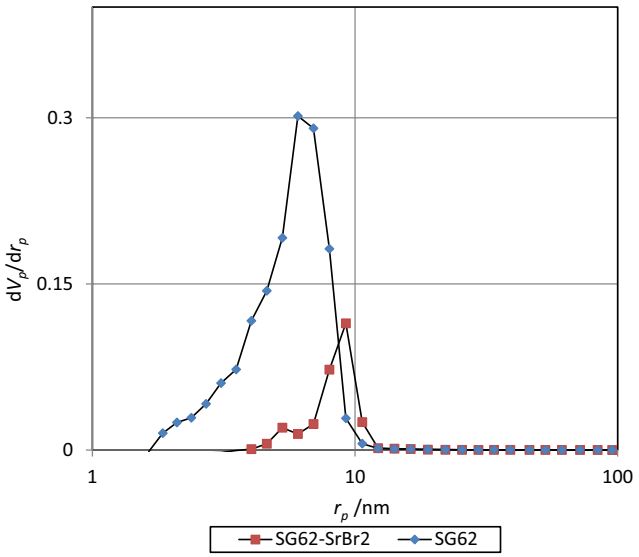

Fig. 2. Pore size distribution of silica gel SG62 (blue) and composite SG62/$SrBr_2$ 58 wt.% (red) obtained by BJH method from nitrogen desorption isotherm at 77 K. (For interpretation of the references to colour in this figure legend, the reader is referred to the web version of this article.)

$$SC_{BET} = \frac{V_{p_{matrix}} - V_{p_{composite}}}{V_{p_{matrix}} + \frac{1}{\rho_{salt}}}$$

The salt content of the anhydrous composite calculated from the pore volumes equal to 59 wt.%, is fully consistent with those derived from the mass of composite or from X ray fluorescence, which means that the salt is mainly incorporated into the pores of silica.

Fig. 3(a) gives an overview of the cross-section of different particles. Fig. 3(b) shows the cross-section of one particle. Locally, and more specifically in the central area of the particle, some small crystals tend to form, possibly revealing the in-depth character of the impregnation process. This visual observation is further confirmed by EDX mapping of Fig. 3c, where Sr and Br are evidenced in the overall cross-section of the particle. Furthermore, the salt content seems to be even slightly higher in the central area of the particle than in the peripheral area. This is of particular interest, since it is likely to favor the material stability. In addition, none of the particles of Fig. 3a correspond to crystallite of $SrBr_2$: all the particles contain Si, Sr and Br elements and no free standing $SrBr_2$ crystallite can be found.

In-depth EDX analyses are given in Fig. 4. For several particles, EDX spectra were acquired on selected areas of the cross-section, to evidence possible differences, as suggested by Fig. 4a. Fig. 4b gives the average chemical analysis based on these spectra. Some discrepancies are observed in the EDX analysis, compared to XRF: they are due to particle heterogeneities and to the fact that the Kα peak of Si and Lα peak of Sr are close to each other. Local EDX analysis gives 53 wt.% $SrBr_2$ for square 1 and 60 wt.% $SrBr_2$ for square 5, assuming that SG62 is stoichiometric SiO_2. This is nevertheless acceptable to appreciate the intra-particle homogeneity. The salt is located all over the particles of silica gel and the composition at the border of the particle is comparable with that at the center of the particle. No crystallite of salt is observed in the sample, either at the surface of silica particle or in the inter-particle porosity which indicates that the impregnation process is particularly effective in embedding the salt into the pores of silica.

The particle size distribution was measured by laser diffraction. In comparison to the pure silica gel (Fig. 5) no small particle of silica with a diameter lower than 10 μm was observed in the composite which may result from an agglomeration of the finest particles during the synthesis of composite. The results also highlight a small increase of the particle size of the composite compared to pure silica gel, with Dv50, the diameter for which 50% of the grains in volume are smaller, switching from 145 ± 5 μm to 178 ± 5 μm.

The water vapor sorption behavior of the composite was evaluated for temperatures ranging from 20 °C to 80 °C on a dynamic vapor sorption apparatus (Fig. 6). Considering a given isotherm, a first mass uptake is observed with increasing pressure, followed by a plateau, then a second increase of the adsorbed mass occurs, followed by a plateau or by a low slope curve (depending on the temperature). At 20 °C and 30 °C for high water vapor partial pressures, another increase of the adsorbed mass is observed. Similarly, X ray diffraction patterns were recorded by varying the temperature, enabling us to understand the behavior of the salt in this composite (Fig. 7). In order to determine the structure at the highest water contents, the material was first hydrated until 0.69 g/g before conducting these X-ray diffraction experiments.

Before recording XRD diagram, SG62/$SrBr_2$ 58 wt.% composite is exposed for about 70 h to a saturated water atmosphere in order to prepare a composite with the highest hydration rate. Then, XRD diagrams are recorded by increasing temperature from 30 to 160 °C. At 30 °C, the X ray diffraction pattern of the composite presents XRD peaks, the assignment of which is consistent with the presence of the hexahydrate form of $SrBr_2$. The low intensity of those XRD peaks indicates that $SrBr_2$ hexahydrate is present in the composite in small amount while the main part of the salt is confined into the pores of silica as amorphous or partially solubilized salt. The high intensity of the peak at $2\theta = 40°$ in comparison to the pattern of the $SrBr_2$ hexahydrate suggests that the different hydrates of $SrBr_2$ coexist in the sample. Upon increasing the temperature, a dehydration process of $SrBr_2$ takes place, as observed by XRD. While the XRD peaks of the hexahydrate form of $SrBr_2$ are clearly observed in the range 40-50 °C, the XRD pattern of the monohydrate form of $SrBr_2$ is obtained from 60 to 150 °C. Finally, the anhydrous form of $SrBr_2$ is evidenced by XRD at 160 °C. Upon decreasing the temperature back to 30 °C, the XRD pattern displays mainly the XRD peaks of the hexahydrate form of $SrBr_2$ with minor peaks of the monohydrate and anhydrous forms of $SrBr_2$.

These analyses enable us to understand the sorption mechanism of water vapor on composite SG62/$SrBr_2$: the first step corresponds to the chemical reaction of $SrBr_2$ from the anhydrous to the monohydrate: $SrBr_{2(s)} + H_2O_{(v)} \leftrightarrow SrBr_2{\cdot}H_2O_{(s)}$. The second step represents the chemical reaction of $SrBr_2$ from monohydrate to

Table 2
Structural characteristics of silica gel SG62 and composite silica gel/$SrBr_2$: specific surface area, total pore volume and average pore diameter obtained from BET analysis and primary mesopore volume, micropore volume and external surface area calculated from α_s-plot analysis of the nitrogen adsorption isotherm at 77 K.

	Specific surface area (m^2/g)	Total pore volume (cm^3/g)	Average pore diameter (nm)	Primary mesopore volume (cm^3/g)	Micropore volume (cm^3/g)	External surface area (m^2/g)
SG62	320	1.14	14	1.13	0	1.93
SG62/$SrBr_2$ 58 wt.%	62	0.33	21	0.32	0	0.99

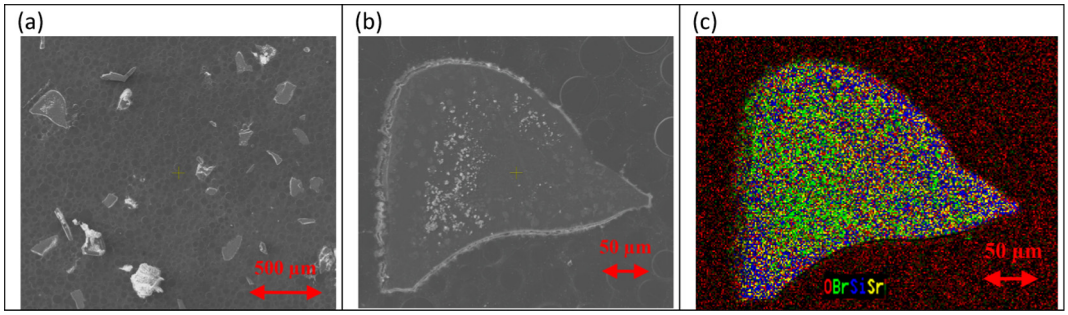

Fig. 3. cross-sectional views of SG62/$SrBr_2$ 58 wt.% composite: (a) SEM image through several particles; (b) SEM image through one single particle; (c) EDX mapping through the particle shown in (b).

hexahydrate: $SrBr_2{\cdot}H_2O_{(s)} + 5\ H_2O_{(v)} \leftrightarrow SrBr_2{\cdot}6H_2O_{(s)}$. Both plateaus with a very small mass uptake correspond to a slight sorption of water on composite. The last mass uptake observed at 20 °C and 30 °C should be representative of absorption in solution of $SrBr_2$.

Fig. 8 shows the water vapor isotherms of silica gel/$SrBr_2$ composite represented as a function of the number of moles of water per mole of $SrBr_2$ in the composite. This confirms the sorption mechanism described earlier, since the first plateau corresponds to the adsorption of one mole of water per mole of $SrBr_2$ and the second plateau to the adsorption of six moles of water per mole of $SrBr_2$. The comparison of the water vapor pressures at which the reaction ($SrBr_2{\cdot}H_2O + 5H_2O \leftrightarrow SrBr_2{\cdot}6H_2O$) occurs in the composite and the pressures at which this reaction occurs in the pure salt (named P reaction in Fig. 8) shows that for temperatures lower than 60 °C, the reaction in the composite occurs at the same pressure as in the pure salt. However, for temperature higher than 60 °C, the reaction in the composite occurs at lower pressure than in the pure salt. This shows that even if the chemical behavior of the salt is conserved in the composite, the thermodynamic equilibrium of the reaction is modified by the incorporation of the salt into the pores of the silica gel. Therefore, the thermodynamic equilibrium data of pure salt cannot describe the sorption behavior of the composite.

The pressure of the reaction of the pure $SrBr_2$ salt ($P_{reaction}$) can be obtained by the following equation:

$$P_{reaction}(Pa) = \exp\left(\frac{8114}{T(K)} + 32.65\right)$$

To describe the sorption isotherms of this composite, a mathematical model is found for water vapor pressure up to 7000 Pa. This mathematical model gives the adsorbed mass (g H_2O/g anhydrous composite) in function of the adsorption potential F as defined by Polanyi [45,46] ($F = RTLn(P_s/P)$, with P_s the saturation pressure at temperature T).

For $F \leqslant 2000$ J/mol,

$$m_{ads} = 58.7035 \times \exp\left(-1.5022 \times F^{0.1588}\right)$$

For 2000 J/mol < $F \leqslant 6500$ J/mol,

$$\text{If } P \geqslant P_{reaction}: m_{ads} = 0.245 + 0.4168 \times \left(99970537.5 \times \exp(-14.8725 \times F^{0.0479})\right)$$

$$\text{If } P < P_{reaction}: m_{ads} = 0.0424 + 9997037.5 \times \exp(-14.8725 \times F^{0.0479})$$

For F > 6500 J/mol,

$$m_{ads} = 0.0424 + 9997037.5 \times \exp\left(-14.8725 \times F^{0.0479}\right)$$

This mathematical model gives a good correlation between calculated and experimental data (Fig. 9) with R^2 of 0.9833. This mathematical model enables us to predict the adsorbed mass in conditions of temperature and pressure different than those experimentally tested. This is important for simulation work; for example, to evaluate the performance of this material in different systems (open or closed). It is also useful in studying the impact of conditions variation on the composite performances.

In order to evaluate the heat storage performance of this composite for solar space heating application, the energy storage density is evaluated between 30 °C and 80 °C at 12.5 mbar (conditions representative of heat storage systems for this kind of application). The experimental cycle loading lift of this composite in these conditions is 0.22 g H_2O/g anhydrous composite. The integration of the heat flow signal with the correction of the crucible and sample heating is 827 J/g of anhydrous composite which corresponds to an energy storage capacity of 230 W h/kg of anhydrous composite and an energy storage density of 203 kW h/m^3 of packing anhydrous composite (the experimental packing density is 885 kg/m^3).

Based on the mathematical model described earlier, one can calculate the cycle loading lift for other conditions. For example, if we consider a storage system working between 40 °C and 80 °C at 12.5 mbar, the calculated cycle loading lift is 0.21 g H_2O/g anhydrous composite, which corresponds to an energy storage density of 191 kW h/m^3 (keeping the same heat of sorption as previously). Provided the adsorption/desorption conditions allow the reaction $SrBr_2{\cdot}H_2O + 5\ H_2O \leftrightarrow SrBr_2{\cdot}6H_2O$ to occur, a change of water vapor pressure does not change the storage capacity (Fig. 10). For example, when considering adsorption conditions at 30 °C and 872 Pa (P_{sat} at 5 °C), corresponding to dry cold air in wintertime, and desorption conditions at 80 °C and 2196 Pa (P_{sat} at 19 °C), corresponding to humid hot air in summertime, the calculated storage capacity is 0.21 g H_2O/g anhydrous composite; when considering adsorption conditions at 30 °C and 611 Pa (P_{sat} at 0 °C), corresponding to very dry cold air in wintertime, and desorption conditions at 80 °C and 2982 Pa (P_{sat} at 24 °C), corresponding to very humid hot air in summertime, the calculated cycle loading lift remains 0.21 g H_2O/g anhydrous composite. Thanks to the chemical sorption behavior of this composite, the cycle loading lift remains constant in a wide range of conditions.

It is interesting to compare the energy storage densities of composite and pure salt. Between 30 °C and 80 °C at 12.5 mbar, the reaction $SrBr_2{\cdot}6H_2O \leftrightarrow SrBr_2{\cdot}H_2O + 5\ H_2O$ occurs. This reaction corresponds to a mass exchange of 0.36 g H_2O/g $SrBr_2$. In these conditions the mass exchange of the composite is 0.22 g H_2O/g anhydrous composite, which corresponds to 0.38 g H_2O/g $SrBr_2$ in the composite. The mass exchange in the composite is mostly due to the chemical reaction of the salt. The experimental porosity (void space between particles) of $SrBr_2{\cdot}6H_2O$ (400 µm) is 0.68, which means that the energy storage density of the salt is

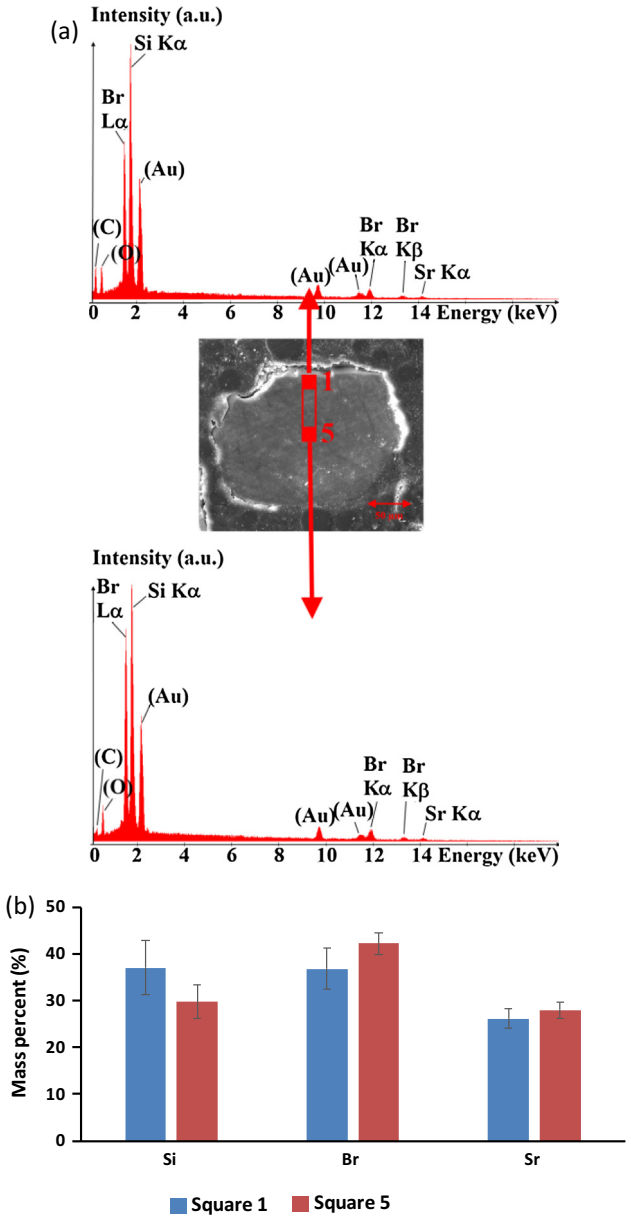

Fig. 4. EDX analyses of selected areas of the particle cross-section: (a) Definition of studied areas and corresponding spectra. Squares 1 and 5 were obtained based on a rectangle of aspect ratio 10:1 inscribed in the cross-section. "Square 1" denotes the first square fully inside the particle and "Square 5" denotes the 5th square from the side. The peaks of gold originate from the conductive layer: they are not accounted for in the homogeneity analysis. The carbon and oxygen peaks were also discarded; (b) Comparison of the EDX analyses realized in a square at the border of the particle (square 1) and in a square at the center of the particle (square 5), results based on 4 particles results. Oxygen is removed from the total due to weak peaks (i.e. 100% refers to Si, Sr and Br). (For interpretation of the references to colour in this figure legend, the reader is referred to the web version of this article.)

201 kW h/m^3 of bulk $SrBr_2{\cdot}6H_2O$, much lower than the crystallographic energy storage densities of 629 kW h/m^3 of $SrBr_2{\cdot}6H_2O$ Taking into account the porosity of the material bed, the energy storage densities of the salt and of the composite are close.

Adding to these promising adsorption results, this composite silica gel/$SrBr_2$ presents an excellent stability over 14 successive sorption/desorption cycles (Fig. 11). These results show that the pores of silica is able to create a stabilizing environment for the salt through specific interactions and confinement effect.

Kinetics is also an important parameter when choosing a heat storage material. The comparison of the hydration tests between

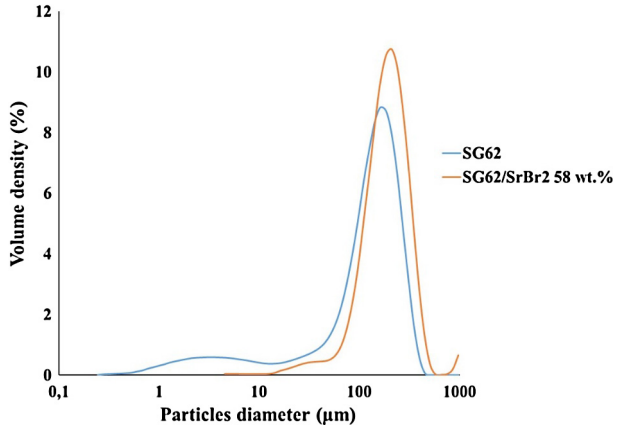

Fig. 5. Comparison of the particle size distribution of the SG62/$SrBr_2$ 58 wt.% composite (orange line) and the pure silica gel SG62 (blue line).

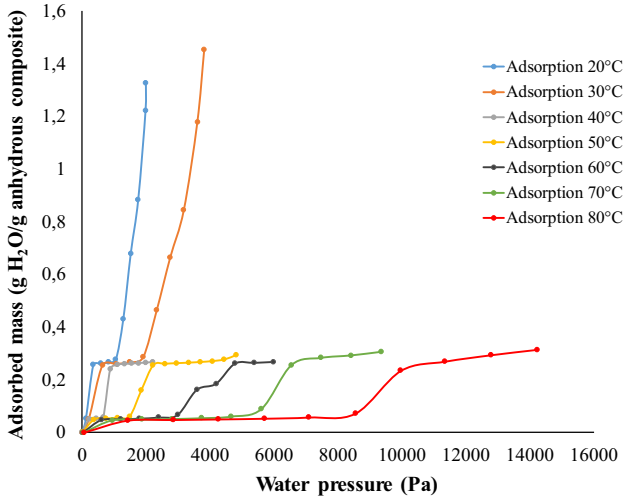

Fig. 6. Water vapor sorption isotherms of SG62/$SrBr_2$ at 58 wt.%.

80 °C and 30 °C at 12.5 mbar of pure $SrBr_2$ and composite SG62/$SrBr_2$ 58 wt.% (Fig. 12) shows that the hydration step is faster for the composite than for $SrBr_2$. Diffusion is not altered by the incorporation of the salt into the pores of the matrix, the access to the salt is even enhanced compared to the pure salt. Particle size also influenced the kinetics as particles of $SrBr_2$ are larger (around 400 µm) compared to those of SG62/$SrBr_2$ 58 wt.% (around 180 µm). The average sorption rate was $1.83 \cdot 10^{-3}$ mg H_2O/g s (mean value between 10 and 40 h) for $SrBr_2$ and $2.91 \cdot 10^{-3}$ mg H_2O/g s (between 5 and 15 h) for SG62/$SrBr_2$ 58 wt.%.

Most advanced technologies in terms of reactor for seasonal thermochemical storage are based on thin-layer solid beds using humid air as heat and mass carrier medium. This configuration allows efficient heat and mass transfer (compared to closed reactors with integrated heat exchanger as part of a water loop connected to the solar collectors or to heat emission system). The present composite material based on $SrBr_2$ and silica gel was tested in a laboratory scale open sorption prototype with a humid air flow rate of 215 L/min. The tests were run on 245 g composite with a 10 mm height layer in the column. The time of the experiment was around 4 h, the test was stopped when the sorption process extent of reaction reached 0.68. At 30 °C and 12.5 mbar, the maximum specific thermal power of 200 W/kg composite and the mean specific thermal power of 92 W/kg composite were obtained. The absolute sorption rate at 65% of equilibrium water

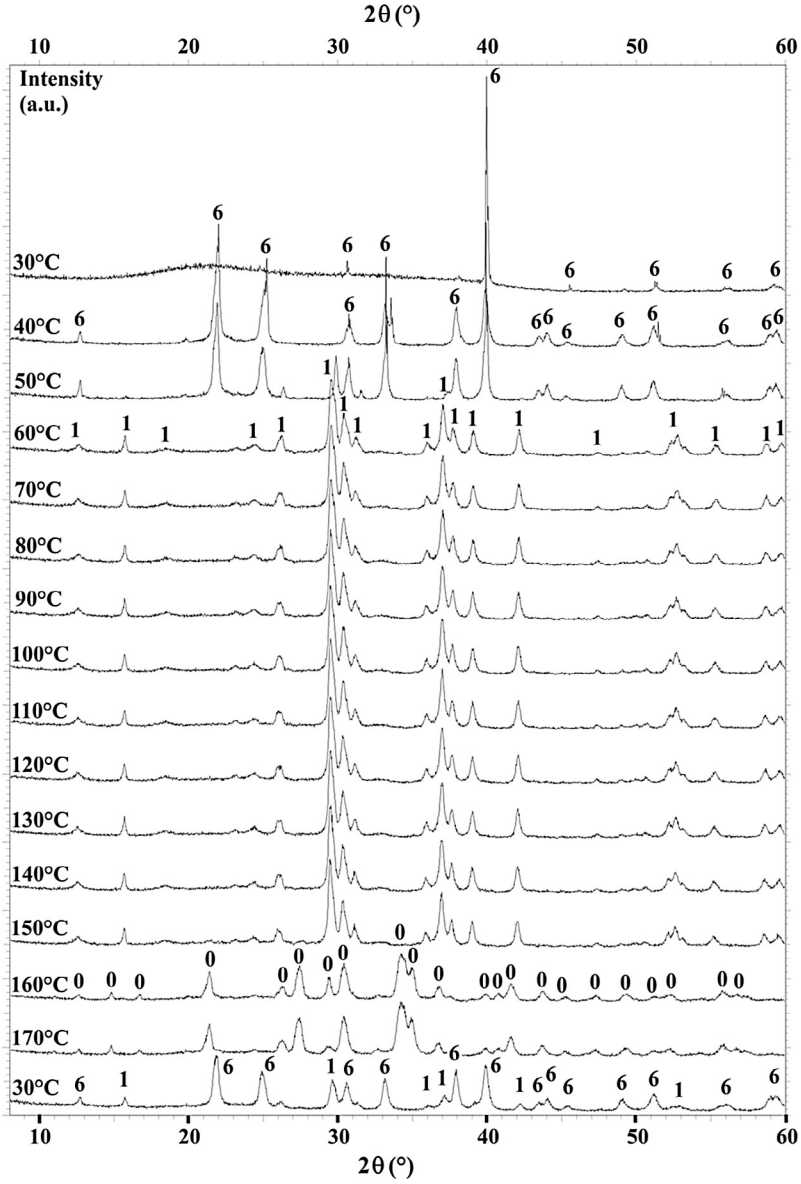

Fig. 7. X ray diffraction patterns of composite SG62/$SrBr_2$ from 30 °C to 170 °C, the composite is initially hydrated at 0.69 g/g. "0", "1" and "6" represent the XRD pattern of the anhydrous, monohydrate and hexahydrate forms of $SrBr_2$, respectively.

uptake was 3 mg H_2O/s, which corresponds to a sorption rate of $12.4 \cdot 10^{-3}$ mg H_2O/g s much higher than the rates obtained in the thermobalance equipment. All these results will be presented in details in a future publication. In open sorption devices, the material is in direct contact with humid air and thus heat transfer is not limitative.

5. Conclusion

A new composite material based on silica gel and strontium bromide was synthesized and characterized to evaluate the possibility of its use for heat storage application. An original synthesis protocol was proposed to enhance both sorption capacity (thanks to high salt content) and cycling stability compared to reported composite materials. A high salt content of 58 wt.% was reached. The structural characterization proves that the salt is homogeneously distributed into the pores of the silica gel and not onto its surface. This composite presents promising cycle loading lift of 0.22 g H_2O/g anhydrous composite (between 30 °C and 80 °C at 12.5 mbar) which corresponds to a high energy storage capacity of 230 W h/kg of anhydrous composite and a high energy storage density of 203 kW h/m^3 of packed bed anhydrous composite. The water vapor sorption isotherms were measured between 20 °C and 80 °C and the sorption mechanism was determined. A mathematical model enabled us to correctly represent the experimental data and hence to predict the sorption behavior of the composite in other conditions. Due to the chemical behavior of this composite for water sorption, the energy storage density remains almost constant in a large range of conditions. This should ensure its stable behavior when used in a complete system likely to work in variable boundary conditions (e.g. variable temperature at the solar collectors outlet). This silica gel/$SrBr_2$ composite has a good stability over 14 successive sorption/desorption cycles. The performances of this new composite overpasses those of the reported composites and particularly zeolite 13X/$MgSO_4$ which obtained only 166 kW h/m^3 whereas the composite silica gel/$SrBr_2$ obtained 203 kW h/m^3 with a lower desorption temperature (80 °C for the present study compared to 150 °C for zeolite 13X/$MgSO_4$ composite). The sorption kinetics of silica gel/$SrBr_2$ 58 wt.% composite was enhanced

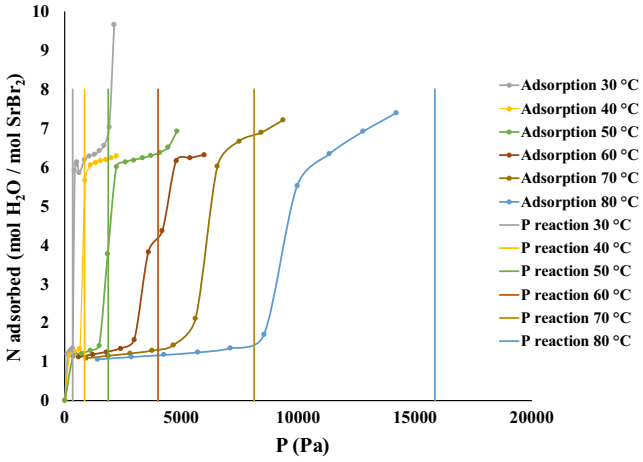

Fig. 8. Comparison between water vapor isotherms of SG62/$SrBr_2$ represented versus the number of moles of water adsorbed per mole of $SrBr_2$. The pressures at which the chemical reaction $SrBr_2{\cdot}H_2O + 5\ H_2O \leftrightarrow SrBr_2{\cdot}6H_2O$ occurs for pure salt are indicated by solid vertical lines.

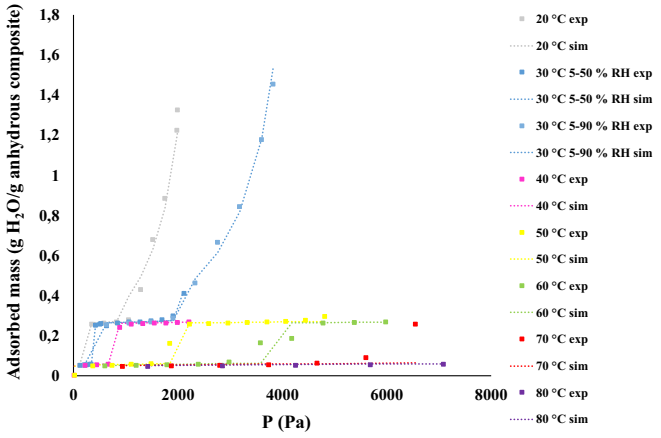

Fig. 9. Comparison between experimental (squares) and simulated data (discontinuous line) for the water vapor sorption isotherms of composite SG62/$SrBr_2$.

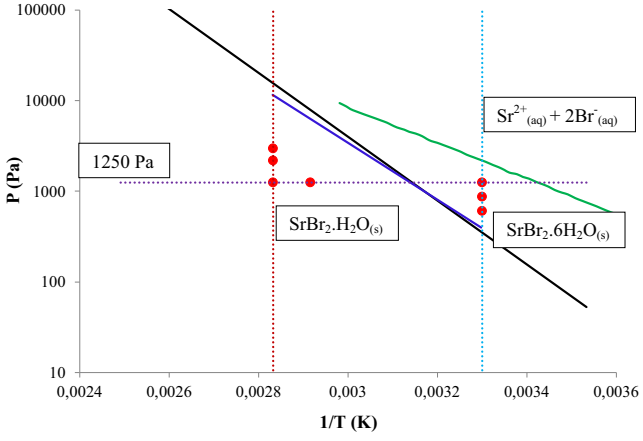

Fig. 10. Equilibrium curve of monohydrate to hexahydrate $SrBr_2$ reaction with water in the pure salt (continuous black line) and in the composite SG62/$SrBr_2$ 58 wt.% (continuous blue line) and dissolution curve of $SrBr_2$ (continuous green line, extracted from [38]) in the Clausius-Clapeyron diagram and conditions of temperature and water vapor pressure used in thermochemical heat storage system (discontinuous lines and red points). (For interpretation of the references to colour in this figure legend, the reader is referred to the web version of this article.)

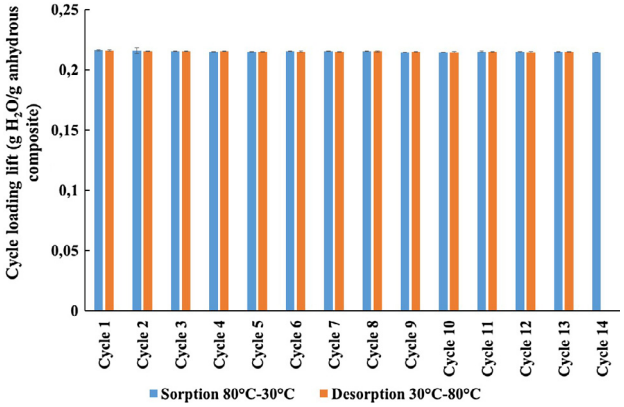

Fig. 11. Stability of SG62/$SrBr_2$ at 58 wt.% under successive sorption/desorption cycles.

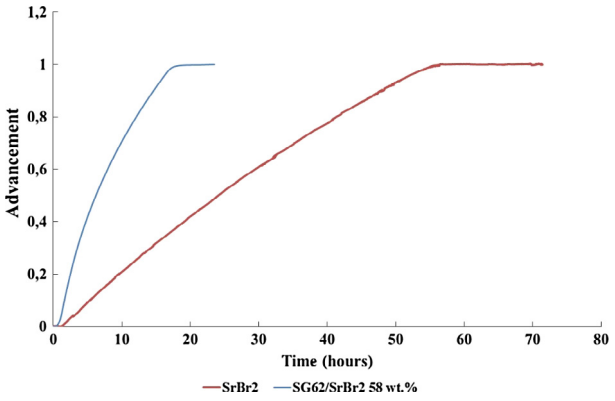

Fig. 12. Comparison of hydration kinetics of $SrBr_2$ (red) and SG62/$SrBr_2$ 58 wt.% (blue), initial conditions: 80 °C and 12.5 mbar, final conditions: 30 °C and 12.5 mbar.

compared to pure strontium bromide. Test on a laboratory scale open type reactor gives a specific thermal power of 200 W/kg and a mean specific thermal power of 92 W/kg at 30 °C and 12.5 mbar for an extent of reaction of 0.68. These performance data show that the used of approximately 13,000 kg (18 m^3) of such a composite would be necessary to store and provide heat for an annual heat demand of 3000 kW h for space heating while the reactor should contain between 10 and 20 kg of composite for providing a 2 kW thermal power (average maximum thermal power in passive one-family dwelling in Belgium).

Further test results on the laboratory scale prototype will be presented in a future paper.

This high energy storage density, the good stability under successive sorption/desorption cycles, the mechanism of sorption and the fact that the salt remains in a solid (crystalline) state in the composite in the conditions of use of a heat storage system make this composite silica gel/$SrBr_2$ a very promising candidate for heat storage application.

Acknowledgements

The authors gratefully acknowledge the financial support of the European Commission within the FP7 program under grant No. 295775 (Project ENER/FP7EN/295775/"Sotherco").

References

[1] Directive 2010/31/UE. Nearly Zero-Energy Building; 2010.
[2] Colclough S, McGrath T. Net energy analysis of a solar combi system with Seasonal Thermal Energy Store. Appl Energy 2015;147:611–6. http://dx.doi.org/10.1016/j.apenergy.2015.02.088.

[3] Tulus V, Boer D, Cabeza LF, Jiménez L, Guillén-Gosalbez G. Enhanced thermal energy supply via central solar heating plants with seasonal storage: a multi-objective optimization approach. Appl Energy 2016;181:549–61. http://dx.doi.org/10.1016/j.apenergy.2016.08.037.

[4] Sibbitt B, McClenahan D, Djebbar R, Thornton J, Wong B, Carrier J, et al. The performance of a high solar fraction seasonal storage district heating system – five years of operation. Energy Procedia 2012;30:856–65. http://dx.doi.org/10.1016/j.egypro.2012.11.097.

[5] N'Tsoukpoe KE, Liu H, Le Pierrès N, Luo L. A review on long-term sorption solar energy storage. Renew Sustain Energy Rev 2009;13(9):2385–96. http://dx.doi.org/10.1016/j.rser.2009.05.008.

[6] Aydin D, Caseay SP, Riffat S. The latest advancements on thermochemical heat storage systems. Renew Sustain Energy Rev 2015;41:356–67. http://dx.doi.org/10.1016/j.rser.2014.08.054.

[7] N'Tsoukpoe KE, Schmidt T, Rammelberg HU, Watts BA, Ruck WKL. A systematic multi-step screening of numerous salt hydrates for low temperature thermochemical energy storage. Appl Energy 2014;124:1–16. http://dx.doi.org/10.1016/j.apenergy.2014.02.053.

[8] Trausel F, de Jong A-J, Cuypers R. A review on the properties of salt hydrates for thermochemical storage. Energy Procedia 2014;48:447–52. http://dx.doi.org/10.1016/j.egypro.2014.02.053.

[9] Lefebvre D, Tezel FH. A review of energy storage technologies with a focus on adsorption thermal energy storage processes for heating applications. Renew Sustain Energy Rev 2017;67:116–25. http://dx.doi.org/10.1016/j.rser.2016.08.019.

[10] Solé A, Martorell I, Cabeza LF. State of the art on gas-solid thermochemical energy storage systems and reactors for building applications. Renew Sustain Energy Rev 2015;47:386–98. http://dx.doi.org/10.1016/j.rser.2015.03.077.

[11] Dicaire D, Handan Tezel F. Regeneration and efficiency characterization of hybrid adsorbent for thermal energy storage of excess and solar heat. Renewable Energy 2011;36:986–92. http://dx.doi.org/10.1016/j.renene.2010.08.031.

[12] Yan T, Wang R, Li T, Wang L, Ishuga T. A review of promising candidate reactions for chemical heat storage. Renew Sustain Energy Rev 2015;43:13–31. http://dx.doi.org/10.1016/j.rser.2014.11.015.

[13] Courbon E. PhD Thesis. Etude du stockage d'énergie thermique d'origine solaire par réaction thermochimique; 2016.

[14] Solé A, Fontanet X, Barranache C, Martorell I, Fernandez AI, Cabeza LF. Parameters to take into account when developing a new thermochemical energy storage system. Energy Procedia 2012;30:380–7. http://dx.doi.org/10.1016/j.egypro.2012.11.045.

[15] Whiting GT, Grondin D, Stosic D, Bennici S, Auroux A. Zeolite-$MgCl_2$ composites as potential long-term heat storage materials: influence of zeolite properties on heats of water sorption. Sol Energy Mater Sol Cells 2014;128:289–95. http://dx.doi.org/10.1016/j.solmat.2014.05.016.

[16] Richter M, Bouché M, Linder M. Heat transformation based on $CaCl_2/H_2O$ – Part A: closed operation principle. Appl Therm Eng 2016;102:615–21. http://dx.doi.org/10.1016/j.applthermaleng.2016.03.076.

[17] Lele A Fopah, Kuznik F, Opel O, Ruck WKL. Performance analysis of a thermochemical based heat storage as an addition to cogeneration systems. Energy Convers Manage 2015;106:1327–44. http://dx.doi.org/10.1016/j.enconman.2015.10.068.

[18] De Jong A-J, Trausel F, Finck C, van Vliet L, Cuypers R. Thermochemical heat storage – system design issues. Energy Procedia 2014;48:309–19. http://dx.doi.org/10.1016/j.egypro.2014.02.036.

[19] Kuznik F, Johannes K, Obrecht C. Chemisorption heat storage in buildings: state-of-the-art and outlook. Energy Build 2015;106:183–91. http://dx.doi.org/10.1016/j.enbuild.2015.07.002.

[20] Aristov Y, Tokarev M, Cacciola G, Restuccia G. Selective water sorbents for multiple applications, 1-$CaCl_2$ confined in mesopores of silica gel: sorption properties. React Kinetics Catal Lett 1996;59(2):325–33. http://dx.doi.org/10.1007/BF02068130.

[21] Aristov Y, Tokarev M, Restuccia G, Cacciola G. Selective water sorbents for multiple applications, 2-$CaCl_2$ confined in micropores of silica gel: sorption properties. React Kinetics Catal Lett 1996;59(2):335–42. http://dx.doi.org/10.1007/BF02068131.

[22] Demir H, Mobedi M, Ülkü S. A review on adsorption heat pump: problems and solutions. Renew Sustain Energy Rev 2008;12:2381–403. http://dx.doi.org/10.1016/j.rser.2007.06.005.

[23] Wongsuwan W, Kumar S, Neveu P, Meunier F. A review of chemical heat pump technology and applications. Appl Therm Eng 2001;21:1489–519. http://dx.doi.org/10.1016/S1359-4311(01)00022-9.

[24] Yu N, Wang LW, Wang LW. Sorption thermal storage for solar energy. Prog Energy Combust Sci 2013;39:489–514. http://dx.doi.org/10.1016/j.pecs.2013.05.004.

[25] Vasiliev LL, Kanonchik LE, Antukh AA, Kulakov AG. NaX Zeolite, active carbon fibre and $CaCl_2$ ammonia reactors for heat pumps and refrigerators. Adsorption 1996;2:311–61.

[26] Wu H, Wang S, Zhu D. Effects of impregnating variables on dynamic sorption characteristics and storage properties of composite sorbent for solar heat storage. Sol Energy 2007;81:864–71. http://dx.doi.org/10.1016/j.solener.2006.11.013.

[27] Gordeeva LG, Glaznev IS, Savchenko EV, Malakhov VV, Aristov YI. Impact of phase composition on water adsorption on inorganic hybrids "salt/silica". J Colloid Interface Sci 2006;301:685–91. http://dx.doi.org/10.1016/j.jcis.2006.05.009.

[28] Simonova IA, Freni A, Restuccia G, Aristov YI. Water sorption on composite «silica modified by calcium nitrate». Microporous Mesoporous Mater 2009;122:223–8. http://dx.doi.org/10.1016/j.micromeso.2009.02.034.

[29] Tretiak CS, Abdallah N. Sorption and desorption characteristics of a packed bed of clay-$CaCl_2$ desiccant particles. Sol Energy 2009;83:1861–70. http://dx.doi.org/10.1016/j.solener.2009.06.017.

[30] Jänchen J, Ackermann D, Wriler E, Stach H, Brösicke W. Calorimetric investigation on zeolites, AlPO4's and $CaCl_2$ impregnated attapulgite for thermochemical storage of heat. Thermochim Acta 2005;434:37–41. http://dx.doi.org/10.1016/j.tca.2005.01.009.

[31] Ji JG, Wang RZ, Li LX. New composite adsorbent for solar-driven fresh water production from the atmosphere. Desalination 2007;212:175–82. http://dx.doi.org/10.1016/j.desal.2006.10.008.

[32] Hongois S, Kuznik F, Stevens P, Roux J-J. Development and characterization of a new $MgSO_4$zeolite composite for long term thermal energy storage. Sol Energy Mater Sol Cells 2011. http://dx.doi.org/10.1016/j.solmat.2011.01.050.

[33] Ristic A, Maucec D, Henninger SK, Kaucic V. New two-component water sorbent $CaCl_2$-FeKIL2 for solar thermal energy storage. Microporous Mesoporous Mater 2012;164:266–72. http://dx.doi.org/10.1016/j.micromeso.2012.06.054.

[34] Zhang YN, Wang RZ, Zhao YJ, Li TX, Riffat SB, Wajid NM. Development and thermochemical characterizations of vermiculite/$SrBr_2$ composite sorbents for low-temperature heat storage. Energy 2016;115:120–8. http://dx.doi.org/10.1016/j.energy.2016.08.108.

[35] Michel B, Mazet N, Mauran S, Stitou D, Xu J. Thermochemical process for seasonal storage of solar energy: characterization and modeling of a high density reactive bed. Energy 2012;47:553–63. http://dx.doi.org/10.1016/j.energy.2012.09.029.

[36] Hennaut S, Thomas S, Davin E, Skrylnyk A, Frère M, André P. Simulation of a vertical ground heat exchanger as low temperature heat source for a closed adsorption seasonal storage of solar heat. Energy Procedia 2014;48:370–9. http://dx.doi.org/10.1016/j.egypro.2014.02.043.

[37] Michel B, Mazet N, Neveu P. Experimental investigation of an innovative thermochemical process operating with a hydrate salt and moist air for thermal storage of solar energy: global performance. Appl Energy 2014;129:177–86. http://dx.doi.org/10.1016/j.apenergy.2014.04.073.

[38] Rambaud G, Mauran S, Mazet N. Modélisation de transfert de vapeur d'eau à faible pression à travers un milieu poreux réactif, Eurotherm Seminar 81, Reactive Heat Transfer in Porous Media, Ecole des Mines d'Albi France, June 4–6 2007.

[39] Lahmidi H, Mauran S, Goetz V. Definition, test and simulation of a thermochemical storage process adapted to solar thermal systems. Sol Energy 2006;80:883–93. http://dx.doi.org/10.1016/j.solener.2005.01.014.

[40] Mauran S, Lahmidi H, Goetz V. Solar heating and cooling by a thermochemical process. First experiments of a prototype storing 60 kW h by a solid/gas reaction. Sol Energy 2008;82:623–36. http://dx.doi.org/10.1016/j.solener.2008.01.002.

[41] Zhao YJ, Wang RZ, Zhang YN, Yu N. Development of $SrBr_2$ composite sorbents for a sorption thermal energy storage system to store low temperature heat. Energy 2016;115:129–39. http://dx.doi.org/10.1016/j.energy.2016.09.013.

[42] Courbon E, Frère M, Heymans N, D'Ans P, Degrez M. Hygroscopic composite material, patent WO2015197788 (A1).

[43] Sayari A, Liu P, Kruk M, Jaroniec M. Characterization of Large-Pore MCM-41 molecular sieves obtained via hydrothermal restructuring. Chem Mater 1997;9:2499–506.

[44] Kruk M, Jaroniec M, Ko CH, Ryoo R. Characterization of the porous structure of SBA-15. Chem Mater 2000;12:1961–8. http://dx.doi.org/10.1021/cm000164e.

[45] Polanyi M. Trans Faraday Soc 1932;28:316.

[46] Polanyi M. Elektrochem 1929;35:431.